This paper is published as part of a *CrystEngComm* themed issue entitled:

New Talent

Showcasing the strength of research being carried out by tomorrow's leaders in the field of crystal engineering in its broadest sense, including crystal growth

Guest Editor and Chair of the *CrystEngComm* Editorial Board:
Professor Neil Champness
University of Nottingham, UK

Published in issue 8, 2010 of *CrystEngComm*

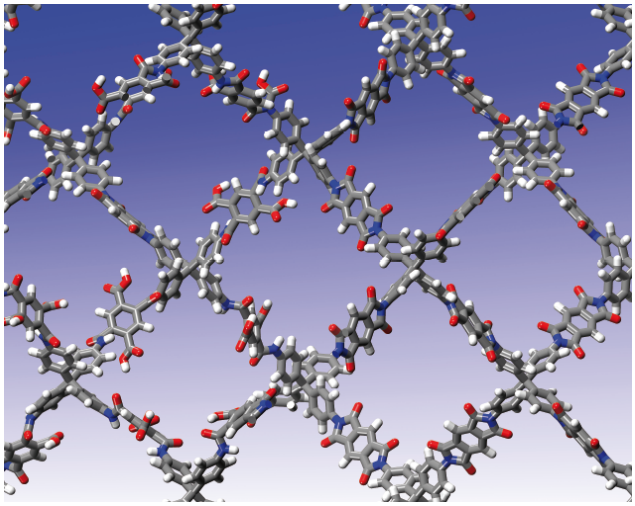

Image reproduced with permission from Abbie Trewin

Other articles published in this issue include:

Dipyrrin based homo- and hetero-metallic infinite architectures
Stéphane A. Baudron, *CrystEngComm*, 2010, DOI: 10.1039/c001020k

Self-assembly of 1,4-cis-polybutadiene and an aromatic host to fabricate nanostructured crystals by π…CH interactions
Silvia Bracco, Angiolina Comotti, Patrizia Valsesia, Mario Beretta and Piero Sozzani
CrystEngComm, 2010, DOI: 10.1039/c002931a

Searching for novel crystal forms by *in situ* high-pressure crystallisation: the example of gabapentin heptahydrate
Francesca P. A. Fabbiani, Demetrius C. Levendis, Gernot Buth, Werner F. Kuhs, Norman Shankland and Heidrun Sowa, *CrystEngComm*, 2010, DOI: 10.1039/b924573a

Postsynthetic diazeniumdiolate formation and NO release from MOFs
Joseph G. Nguyen, Kristine K. Tanabe and Seth M. Cohen
CrystEngComm, 2010, DOI: 10.1039/c000154f

Visit the *CrystEngComm* website for more cutting-edge crystal engineering research
www.rsc.org/crystengcomm

Supramolecular lattice-solvent control of iron(II) spin transition parameters†

Ivan Šalitroš,[ab] Ján Pavlik,[b] Roman Boča,[c] Olaf Fuhr,[a] Chandrasekar Rajadurai[a] and Mario Ruben*[a]

Received 1st February 2010, Accepted 14th April 2010
DOI: 10.1039/c002082f

We report on the synthesis of spin transition compounds **1**, **2** of formula $[Fe(\mathbf{L})_2](A)_2$ (where **L** = 2′,6′-bis(pyrazol-1-yl)-3,4′-bipyridine, A = ClO_4^-—compound **1**; A = BF_4^-—compound **2**) and compound **3** of formula $[Fe(\mathbf{L})(\mathbf{LH})](BF_4)_3 \cdot H_2O \cdot CH_3CN$ (where **LH** = 3-(2,6-bis(pyrazol-1-yl) pyridine-4-yl)-pyridinium(+)). Compounds **1**, **2** and **3** were characterized by single-crystal X-ray diffraction, ESI-ToF mass spectrometry, ^{1}H NMR and elemental analysis. The single-crystal X-ray diffraction study of the counter anion analogues **1** and **2** reveals almost identical molecular structures without any significant presence of intermolecular interactions. However, in the case of compound **3**, the crystal structure reveals supramolecular interactions involving molecular cations, BF_4^- anions and, most importantly, lattice solvent molecules. The presence of solvent water molecules induces the presence of two different types of hydrogen bonding: (i) water molecules interacting with the fluorine atoms of BF_4^- anions and (ii) water molecules interconnecting protonated and nonprotonated nitrogens of pyridine-3-yl substituents of neighboring complex cations. These overall hydrogen bonding pattern between the neighboring iron(II) complex cation moieties is responsible for the formation of a one dimensional (1D) hydrogen bonded zig-zag chain. The magnetic investigations elucidate high temperature spin transition behavior for both anion analogues **1** and **2**, while compound **3** exhibits a lattice-solvent dependency of the temperature-driven spin transition accompanied with stepwise solvent liberation above room temperature. After complete solvent removal the solvent-free compound **3d**, $[Fe(\mathbf{L})(\mathbf{LH})](BF_4)_3$, shows an abrupt spin transition accompanied with thermal hysteresis loop; $T_{1/2(\uparrow)} = 240$ K and $T_{1/2(\downarrow)} = 231$ K, $\Delta T_{1/2} = 9$ K. The Ising-like model that includes two vibrational modes has been applied in a direct fitting of magnetic data. The model recovers the temperature evolution of the χT product functions for all compounds under study, involving also compound **3d** with the thermal hysteresis.

Introduction

One of the main goals in the research field of switchable iron(II) compounds is the steering of the spin transition (ST) parameters in view of potential device applications. The pronounced bistability between high spin (HS) and low spin (LS) states is a very attractive property of ST materials and it was proposed to use such compounds as active units for high capacity memory devices technology,[1,2] display's technology,[3] magnetic resonance imaging contrast agents,[4] molecular sensors, molecular spintronics, *etc.* However, in order to utilize the ST materials in technology, some requirements must be strictly fulfilled:[2] (i) abruptness of transition, (ii) presence of wide thermal hysteresis behaviour ($\Delta T \approx 50$ K), (iii) stability of ST material, and (iv) transition temperature in the room temperature region. With respect to pivotal room temperature switching, so far, only three families of iron(II) spin transition compounds are known.[5] From the structural point of view, the two main classes of room temperature ST compounds—iron(II) triazoles[6] and 2D-Hoffman type pyrazine networks[7]—are extended coordination polymers. The third class of the group of iron(II)-bis(pyrazol-*n*-yl)pyridine complexes ($n = 1$ or 3)[8] is of molecular character enabling the use of spin transition units in single-molecule devices of few nanometre dimensions. The last class is covered also by some other tridentate ligands, like pyridine-bis(benzimidazole) and pyridine-tris(benzimidazole).[9]

Systematic synthetic substitution in 4′-position of the pyridine ring of the bis(pyrazol-1-yl)pyridine (1-bpp) ligand moiety has been shown to be a useful design tool leading to a systematic increase of the spin transition temperatures partially above room temperature. Thus, our group has shown that by introduction of various functionalized groups *i.e.* 4-cyanophenyl,[8b] 4-ethynylphenyl-ethanethioate,[8c] iodo-[8d] and 4-hydroxyphenyl[8d] warrants for steering of the ST properties like abruptness, room temperature transition and cooperativeness.

Moreover, introduction of pyridine-4-yl substituent leads to the linear interconnection of mononuclear iron(II) complexes into a chain-like hydrogen-bonding polymer.[8e] The interconnecting hydrogen bonds are established by the semi-protonation of *p*-pyridine nitrogen atoms of the ligand 4*p*-bpp, forming pyridinium cations that allow self-complementary N^+–H···N to hydrogen bond together with deprotonated pyridines of neighbouring complex units resulting in infinite one-dimensional chains of mononuclear ST Fe(II) centres. The ST of this 1D polymer,

[a]*Institut für Nanotechnologie, Karlsruher Institut für Technologie (KIT), Postfach 3640, 76021 Karlsruhe, Germany. E-mail: mario.ruben@kit.edu*
[b]*Institute of Inorganic Chemistry, Technology and Materials (FCHPT), Slovak University of Technology, 812 37 Bratislava, Slovakia*
[c]*Department of Chemistry (FPV), University of SS Cyril and Methodius, 917 01 Trnava, Slovakia*

† CCDC reference numbers 764304–764306. For crystallographic data in CIF or other electronic format see DOI: 10.1039/c002082f

which is centred exactly at room temperature, is accompanied by a 2 K thermal hysteresis loop and demonstrates the existence of a significant degree of cooperativeness mediated by hydrogen bonds and/or by the methanol molecules trapped in the lattice.

Herein, we report on the spin transition properties of three mononuclear iron(II)-(1-bpp) compounds of the $[Fe(\mathbf{L})_2]^{2+}$-type. The three complexes **1**, **2**, and **3** were characterised by analytical methods (elemental analysis, ESI-ToF mass spectrometry, ^{1}H-NMR) and by single crystal X-ray diffraction analysis. The solvent removal of compound **3** was systematically investigated by thermogravimetric investigations. The ST of all three complexes was studied by variable-temperature magnetic susceptibility measurements. In the case of compounds **1** $[Fe(\mathbf{L})_2](ClO_4)_2$ and **2** $[Fe(\mathbf{L})_2](BF_4)_2$ (where **L** is 2′,6′-bis(pyrazol-1-yl)-3,4′-bipyridine), the influence of counter anion variation on the magnetic properties was investigated exhibiting ST above room temperature in both cases. Complex **3** of the formula $[Fe(\mathbf{L})(\mathbf{LH})](BF_4)_3\cdot H_2O\cdot CH_3CN$ (where **LH** = 3-(2,6-bis(pyrazolyl-1-yl)pyridine-4-yl)-pyridinium(+)) contains two solvent water molecules per unit cell. The influence of the presence of the lattice-solvent molecules on the ST parameters of complex **3** was investigated in detail, whereby the complete solvent removal, performed *in situ* during the magnetic measurements by four heating/cooling cycles, leads to the loss of the room temperature ST. The desolvated compound **3d** reveals a low-temperature ST exhibiting a 9 K thermal hysteresis.

Experimental

General

Purchased chemicals (3-pyridineboronic acid, $Fe(BF_4)_2\cdot 6H_2O$, $Fe(ClO_4)_2$hydrate, $Pd^0(PPh_3)_4$, Na_2CO_3) were used as received. Tetrahydrofuran, dichloromethane, methanol, acetonitrile and diethyl ether solvents were used without any further purification. Elemental analyses of carbon, hydrogen, and nitrogen were carried out by Vario Micro Cube. ^{1}H and ^{13}C NMR spectra were recorded in a Bruker DPX 300 spectrometer with solvent proton and carbon atoms as an internal standard. Matrix-assisted laser desorption/ionization time-of-flight (MALDI-TOF) mass spectrometric analytical data were acquired on a Voyager-DE PRO Bio spectrometry workstation. Electro-spray ionization times of flight (ESI TOF) mass spectrometric analytical data were acquired on a microOTOF-Q II Bruker. Thermogravimetric analysis (TG) was performed in a He flow at a heating rate of 2.5 K min^{-1} in a Netzsch STA 409 C analyzer.

Synthesis

4-Iodo-2,6-bis(pyrazol-1-yl)pyridine was synthesized following reported procedures.[8b–e]

2′,6′-Bis(pyrazol-1-yl)-3,4′-bipyridine (L). 4-Iodo-2,6-dipyrazolyl-pyridine (1.348 g, 4 mmol), 3-pyridineboronic acid (0.492 g, 4 mmol) and $Pd^0(PPh_3)_4$ (0.46 g, 0.4 mmol, 10%) were suspended in a N_2 gas bubbled solution of tetrahydrofuran and 2 M Na_2CO_3 (aq) (10 cm^3) and heated to 80 °C for 3 days under a nitrogen atmosphere. The mixtures of solvents were removed using a rotary evaporator and remaining residue was treated with water and extracted with CH_2Cl_2 solvent. The separated organic layer was dried over $MgSO_4$ and the solvent was removed by evaporation. The solid residue was at first column chromatographed on silica with CH_2Cl_2/methanol (20 : 1, $R_f = 0.39$) as an eluent. The combined colourless solutions yielded upon evaporation a white powder of compound **L** (0.92 g, yield 80%). ^{1}H NMR (300 MHz, CD_2Cl_2, 25 °C, δ/ppm): $\delta = 9.01$ (t, 1H, 3-Py), 8.68 (dd, 1H, pyridine-3-yl), 8.62 (dd, 2H, pyrazole), 8.1 (s, 2H, 4-pyridine), 8.06 (m, 1H), 7.75 (dd, 2H), 7.44 (q, 1H, pyridine-3-yl), 6.52 (m, 2H). ^{13}C NMR (75 MHz, $CDCl_3$, 25 °C, δ/ppm): 151, 150.8, 150.7, 148.2, 142.5, 134.5, 133.3, 127.2, 123.7, 108.1, 107.2. MALDI-TOF experiment: *m*/*z* (relative intensity of isotopic distribution) = 289.79 (100%), 290.78 (22%), 291.80 (5%); simulation: *m*/*z* (relative intensity of isotopic distribution) = 288.11 (100%), 289.11 (21%), 290.12 (4%). Elemental analysis for $C_{16}H_{12}N_6$ (288.31): found (calc.): C 66.41 (66.66)%; H 4.28 (4.20)%; N 28.29 (29.15)%.

$[Fe(\mathbf{L})_2](ClO_4)_2$ (1). In 100 cm^3 two necked round bottom flask, a solution of **L** (0.1 g, 0.35 mmol) in 50 cm^3 of acetonitrile was deoxygenated under the N_2 flux, warmed up to 60 °C and then a stoichiometric amount (2 : 1) of $Fe(ClO_4)_2$ hydrate (0.044 g, 0.17 mmol) was added. The coordination of ligand **L** took place immediately and the colour of solution turned to red orange. The resulting reaction mixture was stirred at initial conditions (60 °C, N_2 atmosphere) for 3 hours, cooled down to room temperature, and filtered. Orange coloured block-shaped crystals were grown from diffusing the diethyl ether into an acetonitrile solution of the complex under N_2 at room temperature. Calc. for $C_{32}H_{24}Cl_2O_8FeN_{12}$ (831.36 g mol^{-1}). Found (calc.): C 46.16 (46.23)%; H 2.99 (2.91)%; N 20.24 (20.22)%. ESI-TOF MS: $\{[Fe(\mathbf{L})_2]\}^{2+}$ ($FeC_{32}H_{24}N_{12}$) at *m*/*z* = 316.09 (calc. *m*/*z* = 316.08); $\{[Fe(\mathbf{L})_2(ClO_4)]\}^+$ ($FeC_{32}H_{24}N_{12}ClO_4$) at *m*/*z* = 731.13 (calc. *m*/*z* = 731.12); $\{[Fe(\mathbf{L})_2(ClO_4)_2]Na\}^+$ ($FeC_{32}H_{24}N_{12}ClO_4Na$) at *m*/*z* = 885.26 (calc. *m*/*z* = 853.05). ^{1}H NMR (300 MHz, CH_3CN, 25 °C, δ/ppm): 63.70 (pyrazole), 56.31 (4-pyridine), 38.03 (pyrazole), 36.89 (s, pyrazole), 9.16 (1H, pyridine-3-yl), 8.88 (1H, pyridine-3-yl), 8.52 (1H, pyridine-3-yl), 8.20 (1H, pyridine-3-yl). Yield 0.11 g (0.13 mmol, 78%).

Caution. *Although we have experienced no difficulties in handling this compound, metal–organic perchlorates are potentially explosive and should be handled with care in small quantities.*

$[Fe(\mathbf{L})_2](BF_4)_2$ (2). A similar procedure as for **1** was applied using $Fe(BF_4)_2\cdot 6H_2O$ (0.058 g, 0.17 mmol). The crystallisation yielded orange block-shaped crystals. Calc. for $C_{32}H_{24}B_2F_8FeN_{12}$ (806.07 g mol^{-1}) found (calc.): C 46.97 (47.68)%; H 3.01 (3.00)%; N 20.19 (20.85)%. ESI-TOF MS: $\{[Fe(\mathbf{L})_2]\}^{2+}$ ($FeC_{32}H_{24}N_{12}$) at *m*/*z* = 316.08 (calc. *m*/*z* = 316.08); $\{[Fe(\mathbf{L})_2(BF_4)]\}^+$ ($FeC_{32}H_{24}N_{12}BF_4$) at *m*/*z* = 719.15 (calc. *m*/*z* = 731.16). ^{1}H NMR (300 MHz, CH_3CN, 25 °C, δ/ppm): 65.24 (pyrazole), 57.38 (4-pyridine), 38.83 (pyrazole), 37.87 (s, pyrazole), 8.97 (1H, pyridine-3-yl), 8.70 (1H, pyridine-3-yl), 8.16 (1H, pyridine-3-yl), 7.60 (1H, pyridine-3-yl). Yield 0.10 g (0.13 mmol, 74%).

$[Fe(\mathbf{L})(\mathbf{LH})](BF_4)_3\cdot H_2O\cdot CH_3CN$ (3) (where LH^+ = 3-(2,6-bis(pyrazol-1-yl)pyridine-4-yl)-pyridinium(+)). A similar procedure as for **1** and **2** was applied using an excess of $Fe(BF_4)_2\cdot 6H_2O$ (0.087 g, 0.26 mmol, stoichiometric ratio

L : $Fe(BF_4)_2H_2O$ = 2 : 1.5). The crystallisation yielded orange needle-shaped crystals. Calc. for $C_{34}H_{29}B_3F_{12}FeN_{13}O$ (951.94 g mol^{-1}) found (calc.): C 43.58 (42.90)%; H 3.23 (3.07)%; N 19.14 (19.13)%. ESI-TOF MS: $\{[Fe(\mathbf{L})(\mathbf{LH})]\}^{3+}$ ($FeC_{32}H_{25}N_{12}$) at m/z = 211.05 (calc. m/z = 211.06); $\{[Fe(\mathbf{L})(\mathbf{LH})(BF_4)_2]\}^{+}$ ($FeC_{32}H_{25}N_{12}B_2F_8$) at m/z = 807.1682 (calc. m/z = 807.17). ^{1}H NMR (300 MHz, CH_3CN, 25 °C, δ/ppm): 63.06 (pyrazole), 55.58 (4-pyridine), 37.60 (pyrazole), 36.19 (s, pyrazole), 9.45 (1H, pyridine-3-yl), 9.15 (1H, pyridine-3-yl), 8.62 (1H, pyridine-3-yl), 7.91 (1H, pyridine-3-yl). Yield 0.17 g (0.18 mmol, 69%).

Magnetic susceptibility measurements

All herein reported magnetic measurements were performed on a SQUID magnetometer (Quantum Design, model MPMS-XL-5). In all cases, the temperature dependence of the magnetic moment was recorded at B = 0.1 T as an external magnetic field. The temperature sweeping rate was the same for cooling, heating and for the experiments performed on the original and desolvated samples. For **1** and **2**: 2 K min^{-1} (5–200 K), 1 K min^{-1} (200–380 K), 1 K min^{-1} (300–480 K); for solvated compound **3**: 2 K min^{-1} (5–250 K), 1 K min^{-1} (250–380 K); for desolvated compound **3**: 2 K min^{-1} (5–200 K), 1 K min^{-1} (200–280 K), 2 K min^{-1} (280–380 K). Desolvation of compound **3** was obtained *in situ* within the magnetic measurements by four continuous cooling/heating cycles and maintaining the sample in the magnetometer at 380 K for 200 min before every cooling/heating cycle until the last and next to last measurement cycle were identical. Gelatin capsules as sample containers for the measurement in the temperature range 5–380 K were used. In the case of high temperature mode measurement (300–480 K), a special heating setup was used and high temperature sample holder consisted of Quartz glass tube and Teflon filler. The very small diamagnetic contribution of the gelatin capsule and high temperature sample holder had negligible contribution to the overall magnetization, which was dominated by the sample. The diamagnetic corrections of the molar magnetic susceptibilities were applied using Pascal's constants.

Crystal structure determination

Single crystal X-ray diffraction data were collected on a STOE IPDS II diffractometer with graphite monochromated Mo Kα radiation (0.71073 Å). Structure solution and refinement against F^2 were carried out using SHELXS and SHELXL software.[10] Refinement was performed with anisotropic temperature factors for all non-hydrogen atoms (disordered atoms were refined isotropically).

Fitting of magnetic data

The primary magnetic data—the temperature dependence of the magnetic susceptibility—have been directly fitted without any data transformations. The molar magnetic susceptibility consists of the low-spin (LS) and high-spin (HS) contributions along with some paramagnetic impurity (PI):

$$\chi_{mol} = x_{LS} \times \chi_{LS} + x_{HS} \times \chi_{HS} + x_{PI} \times \chi_{PI} \quad (1)$$

where the mole fractions fulfil a normalization $x_{LS} + x_{HS} + x_{PI} = 1$. For the LS and HS state the Curie–Weiss law is to be obeyed, hence:

$$\chi_S = \frac{N_A \mu_0 \mu_B^2}{k} \frac{S(S+1)}{3} \frac{g_S^2}{T - \Theta_S} + \alpha_S \quad (2)$$

where in addition to fundamental physical constants the magnetogyric factor, Weiss constant, and the temperature-independent (van Vleck) term occur. While the mole fraction of the paramagnetic impurity (assumed as a high-spin Fe(III) system) is fixed, the mole fraction x_{HS} is a temperature-dependent quantity determined by a particular model of the spin crossover. Hereafter, the Ising-like model (equivalent to the regular solution model) has been applied as follows.[11] The following equation:

$$x_{HS} = \frac{F(x_{HS})}{1 + F(x_{HS})} \quad (3)$$

is to be iterated starting with $x_{HS}(T_i^{(0)}) = x_{HS}(T_{i-1}^{(n)})$ in the heating mode, and $x_{HS}(T_i^{(0)}) = x_{HS}(T_{i+1}^{(n)})$ in the cooling mode of the data taking ($T_{i-1} < T_i < T_{i+1}$). The factor entering the principal equation reads:

$$F(x_{HS}) = r_{eff} \exp\left[-\frac{\Delta_{eff} - 2J(2x_{HS} - 1)}{kT} \right] \quad (4)$$

This factor involves the parameters of the spin crossover: the energy gap corrected for the zero-point vibrations is proportional to the enthalpy of the spin transition, $\Delta H = R\Delta_{eff}$, the effective degeneracy ratio:

$$r_{eff} = \frac{g_{HS}^{el} \times z_{HS}^{vib}}{g_{LS}^{el} \times z_{LS}^{vib}} = 5\left(\frac{1 - \exp(-h\bar{\nu}_{LS}/kT)}{1 - \exp(-h\bar{\nu}_{HS}/kT)} \right)^{15} \quad (5)$$

is expressed with the help of the electronic and vibrational part, the latter involves two averaged (Einstein-like) vibrational modes $h\bar{\nu}_{LS}$ and $h\bar{\nu}_{HS}$. The parameter J describes the solid-state cooperativeness (not to be confused with the exchange coupling constant). With $J/k > T_{1/2}$ the systems exhibits a thermally induced hysteresis. For $S_{LS} = 0$, $S_{HS} = 2$, and $S_{PI} = 5/2$ ($g_{PI} = 2$) the model involves in total the following free parameters: g_{HS}, α_{LS}, x_{PI}, Θ_{PI}, J, Δ_{eff}, $h\bar{\nu}_{LS}$ and $h\bar{\nu}_{HS}$ which are effective in different temperature windows.

Results and discussion

Synthesis and thermogravimetric studies

Ligand **L**, 2′,6′-bis(pyrazol-1-yl)-3,4′-bipyridine, was obtained as a white powder in 80% yield *via* a Pd-catalyzed Suzuki cross-coupling reaction from ligand 4-iodo-2,6-bis(pyrazol-1-yl)pyridine,[8b–e] with 3-pyridineboronic acid. Compounds **1** and **2** were prepared by the reaction of 2 equivalents of **L** with one equivalent of the respective iron(II) salt in acetonitrile at 60 °C and under the inert atmosphere. Compound **3** was prepared by reaction of 2 equivalents of **L** with 1.5 equivalent of $Fe(BF_4)_2 \cdot 6H_2O$. Single crystals of all three compounds were obtained by diffusing diethyl ether into an acetonitrile solution of the complexes under N_2 atmosphere at room temperature.

Thermogravimetric analysis of **3** was performed in order to investigate the release of the solvent molecules from the crystal structure of compound **3** (Fig. 1). It is shown that the loss of

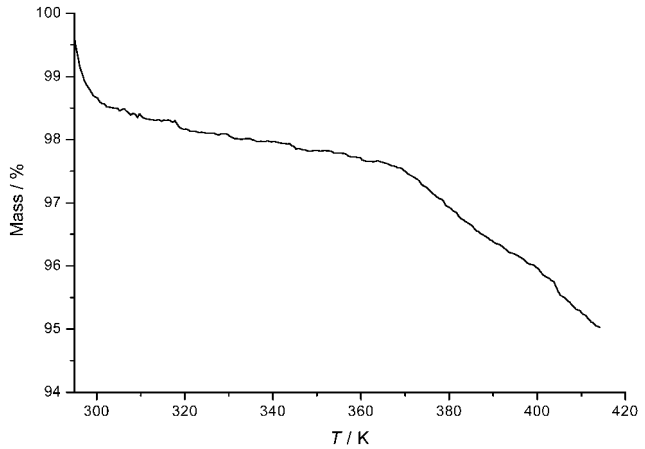

Fig. 1 Thermogravimetric analysis of compound **3** [Fe(**L**)(**L-H**)]$(BF_4)_3 \cdot H_2O \cdot CH_3CN$.

water molecules takes place as a first. A decrease of weight of 2%, corresponding to the loss of one water molecule is observed in the 295–368 K range. The second step occurs in the range of 368–414 K exhibiting a weight decrease of 2.5% and at maximal measured temperature the thermogravimetric curve keeps on showing decreasing character. Expected mass loss for complete removal of acetonitrile from the sample is 4.4% and it will take a place above 414 K. Obviously, complete desolvation should be fully accessible within the temperature range of magnetic measurements.

Crystal structure analysis

Compounds **1** and **2** of the formula $[Fe(\mathbf{L})_2](A)_2$ (A is ClO_4^- for **1**, and BF_4^- for **2**) are in fact counter anion analogues. Both contain the same complex cation $[Fe(\mathbf{L})_2]^{2+}$, but two perchlorate or tetrafluoroborate counter anions, respectively.

The X-ray diffraction studies of compound **1** reveal a monoclinic space group *C*2/*c* exhibiting a unit cell volume V = 6605(2) Å^3 (a = 41.327(8) Å, b = 9.790(2) Å, c = 16.801(3) Å, β = 103.67(3)°; Table 1). The asymmetric unit contains one $[Fe(\mathbf{L})_2]^{2+}$ cation and two perchlorate counter anions (one of them disordered); no solvent molecules are present in the crystal lattice (Fig. 2). The external pyridine-3-yl groups of ligand **L** are not protonated. The coordination environment in the iron(II) metal ion can be described as a distorted octahedron. The complex exhibits Fe–N bond lengths varying from 1.884(4) to 1.976(2) Å (Table 2), which indicate low spin state of iron(II) at 180(2) K.

Compound **2** is isostructural with compound **1** exhibiting the monoclinic *C*2/*c* space group with unit cell parameters of a = 41.196(8) Å, b = 9.874(2) Å, c = 16.528(3) Å, β = 104.03(3)°, V = 6523(2) Å^3 (Table 1). The asymmetric unit contains one $[Fe(\mathbf{L})_2]^{2+}$ cation and two BF_4^- counter anions (one of them disordered); no solvent molecules are present in the crystal lattice and the unit cell contains eight formula units (Fig. 3). The coordination environment in the iron(II) metal ion refers to a tetragonally distorted octahedron and the complex cation exhibits at 180(2) K Fe–N bond lengths varying from 1.892(3) to 1.972(3) Å (Table 2) indicating low spin state of iron(II).

In contrast to compound **2**, the synthesis using a 2 : 1.5 ratio of 2′,6′-bis(pyrazol-1-yl)-3,4′-bipyridine (**L**): $Fe(BF_4)_2 \cdot 6H_2O$ resulted in compound **3** of the formula $[Fe(\mathbf{L})(\mathbf{LH})](BF_4)_3 \cdot H_2O \cdot CH_3CN$ (where **LH** = 3-(2,6-bis(pyrazol-1-yl)pyridine-4-yl)-pyridinium(+)). Single crystal X-ray diffraction reveals that one of the two **L** ligands of the resulting iron(II) compound contains an external pyridine-3-yl ring in its protonated form. In this case the iron(II) complex cation possesses an overall charge

Table 1 Crystal data for compounds **1**, **2** and **3**

	1 $[Fe(\mathbf{L})_2](ClO_4)_2$	**2** $[Fe(\mathbf{L})_2](BF_4)_2$	**3** $[Fe(\mathbf{L})(\mathbf{LH})](BF_4)_3 \cdot CH_3CN \cdot H_2O$
Formula	$C_{32}H_{24}Cl_2FeN_{12}O_8$	$C_{32}H_{24}B_2F_8FeN_{12}$	$C_{34}H_{30}B_3F_{12}FeN_{13}O$
Formula weight/g mol^{-1}	831.38	806.10	952.99
Crystal colour	Red	Red	Red
Temperature/K	180(2)	180(2)	180(2)
Wavelength/Å	0.71073	0.71073	0.71073
Crystal system	Monoclinic	Monoclinic	Monoclinic
Space group	*C*2/*c*	*C*2/*c*	$P2_1/c$
a/Å	41.327(8)	41.196(8)	15.177(3)
b/Å	9.790(2)	9.874(2)	17.0990(19)
c/Å	16.801(3)	16.528(3)	16.797(3)
α/°	90.00	90.00	90.00
β/°	103.67(3)	104.03(3)	111.74(14)
γ/°	90.00	90.00	90.00
V/Å^3	6605(2)	6523(2)	4048.9(11)
Z, $\rho_{calc.}$/g cm^{-3}	8, 1.672	8, 1.642	4, 1.563
μ (Mo-Kα)/mm^{-1}	0.693	0.556	0.477
F(000)	3392	3264	1928
Crystal size/mm	0.25 × 0.20 × 0.04	—	0.48 × 0.22 × 0.17
θ Range for the data collection/°	2.03–25.66	2.04–25.63	1.44–25.63
Final R indices [$I > 2\sigma(I)$][a]	$R_1 = 0.0647$, w$R_2 = 0.1375$	$R_1 = 0.0656$, w$R_2 = 0.1823$	$R_1 = 0.0739$, w$R_2 = 0.2034$
R indices (all data)[a]	$R_1 = 0.1265$, w$R_2 = 0.1617$	$R_1 = 0.0773$, w$R_2 = 0.1924$	$R_1 = 0.0820$, w$R_2 = 0.2111$
Extinction coefficient	0.00169(15)	0.0071(7)	0.0024(10)
GoF on F^2	0.930	1.061	1.046

[a] $R_1 = \sum(F_0 - F_C)/\sum(F_0)$; $wR_2 = \sqrt{\sum\left[w\left(F_0^2 - F_C^2\right)^2\right]/\sum\left[w\left(F_0^2\right)^2\right]}$.

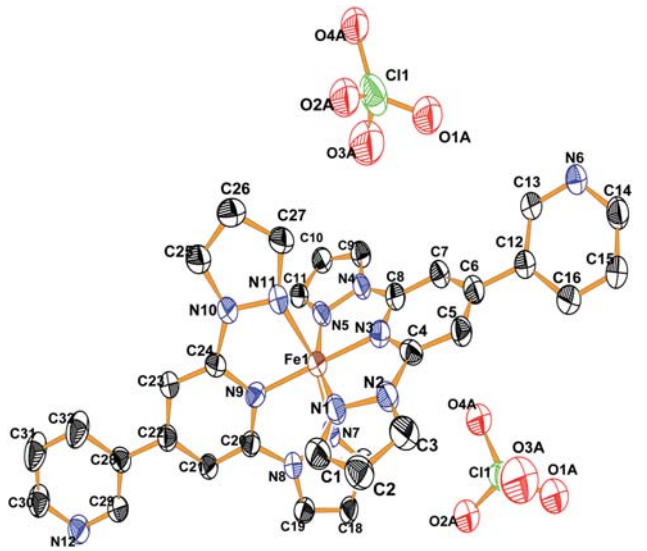

Fig. 2 ORTEP view of the crystal structure of compound **1** $[Fe(\mathbf{L})_2](ClO_4)_2$ (50% probability level of thermal ellipsoids). Bond distances of coordination polyhedron at 180(2) K (in Å): Fe1–N1 = 1.974(5), Fe1–N3 = 1.884(4), Fe1–N5 = 1.976(5), Fe1–N7 = 1.962(5), Fe1–N9 = 1.889(4), Fe1–N11 = 1.966(5).

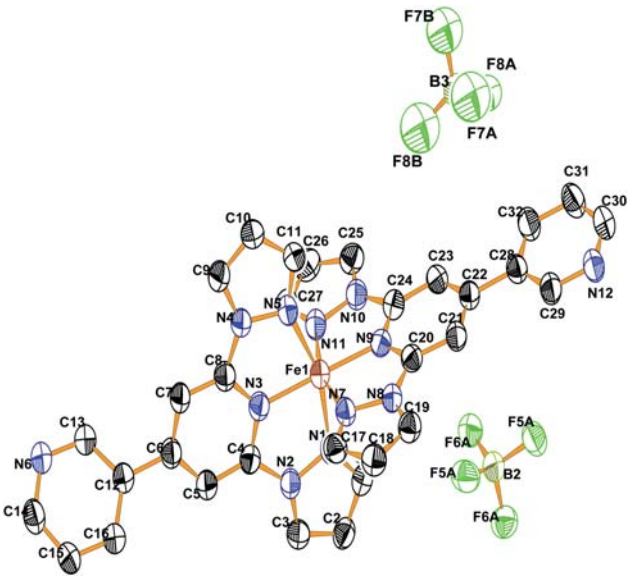

Fig. 3 ORTEP view of the crystal structure of compound **2** $[Fe(\mathbf{L})_2](BF_4)_2$ (50% probability level of thermal ellipsoids). Bond distances of coordination polyhedron at 180(2) K (in Å): Fe1–N1 = 1.972(3), Fe1–N3 = 1.895(3), Fe1–N5 = 1.975(3), Fe1–N7 = 1.968(3), Fe1–N9 = 1.892(3), Fe1–N11 = 1.970(3).

of 3+ counter balanced by three tetrafluroborate counter anions. Additionally, the crystal lattice contains one molecule of acetonitrile and one molecule of water (Fig. 4).

The crystal lattice of compound **3** shows the monoclinic space group $P2_1/c$ with a unit cell volume $V = 4048.9(11)$ Å^3 and cell parameters $a = 15.177(3)$ Å, $b = 17.0990(19)$ Å; $c = 16.797(3)$ Å; $\beta = 117.81(14)°$ (Table 1). The asymmetric unit contains one $[Fe(\mathbf{L})(\mathbf{LH})]^{3+}$ cation, three disordered BF_4^- counter anions, one molecule of CH_3CN and one molecule of water. The coordination environment in the iron(II) metal ion reveals a distorted octahedron. At the temperature of measurement (180 K), Fe^{II}–N distances are in the range 1.890(3)–1.977(3) Å (Table 2), which are characteristic distances for iron(II) coordination centre in the low-spin state. The unit cell contains 4 molecular species of $[Fe(\mathbf{L})(\mathbf{LH}^+)](BF_4)_3 \cdot H_2O \cdot CH_3CN$.

The iron(II) complex moieties are involved in intermolecular interactions with solvent water molecules. One molecule of H_2O inter-connects two neighbouring $[Fe(\mathbf{L})(\mathbf{LH})]^{3+}$ cations *via* hydrogen bonds with protonated and unprotonated nitrogen atoms of pyridine-3-yl substituents ($O1–N6_{protonated} = 2.587$ Å; $O1–N12_{unprotonated} = 2.717$ Å) and forms an infinite one-dimensional hydrogen bonded zig–zag chain along *bc* plane (Fig. 5). In addition, the same molecule of water creates a third hydrogen bond with fluorine atoms (O1–F4A = 2.699 Å). Interestingly, the acetonitrile molecules do not take part in the supramolecular organisation. The C13–N6–C14 bond angle (122.23°) in the pyridinium unit is enlarged in comparison with the respective angle of unprotonated pyridine unit (117.88°).

The hydrogen bonding of both pyridine-3-yl groups causes dramatic deformation of certain angles in the structure of complex cation $[Fe(\mathbf{L})(\mathbf{LH})]^{3+}$ with comparison to the non-protonated structures of compounds **1** and **2**. The molecular angle C14–Fe1–C30, which represents alignment of two coordinated ligands **L** with respect to the iron(II) coordination centre, is almost straight in the case of compounds **1** (178.24°) and **2** (178.47°). However, angle C14–Fe1–C30 in the case of compound **3** is significantly deformed (164.02°) due to the hydrogen bonds between neighbouring complex cations. The other angle deformations were observed also in the case of coordination polyhedra of reported structures (Table 3).

Table 2 Bond distances (in Å, at 180(2) K) of coordination polyhedra of compounds **1**, **2** and **3**

	1	2	3
Fe1–N1	1.974(5)	1.972(3)	1.977(3)
Fe1–N3	1.884(4)	1.895(3)	1.890(3)
Fe1–N5	1.976(5)	1.975(3)	1.975(3)
Fe1–N7	1.962(5)	1.968(3)	1.980(3)
Fe1–N9	1.889(4)	1.892(3)	1.894(3)
Fe1–N11	1.966(5)	1.970(3)	1.957(3)

Magnetic properties

The variable temperature magnetic investigations of **1** and **2** compounds (Fig. 6) were carried out in temperature ranges 5–370 K and 300–485 K (high temperature SQUID option) in both, cooling and heating mode, in order to detect thermal hysteresis effects. Those two analogues of the complex cation $[Fe(\mathbf{L})_2]^{2+}$ exhibit rather similar spin transition properties. The product function χT of compound **1** at 5 K is 0.026 cm^3 mol^{-1} K, which is in accordance with expected value of iron(II) compound in the low-spin state ($S = 0$). Complex **1** shows temperature-independence of the χT product in the range of 30–300 K and the remaining value of 0.309 cm^3 mol^{-1} K at 300 K indicates the presence of traces of paramagnetic Fe^{III} impurities in the sample.

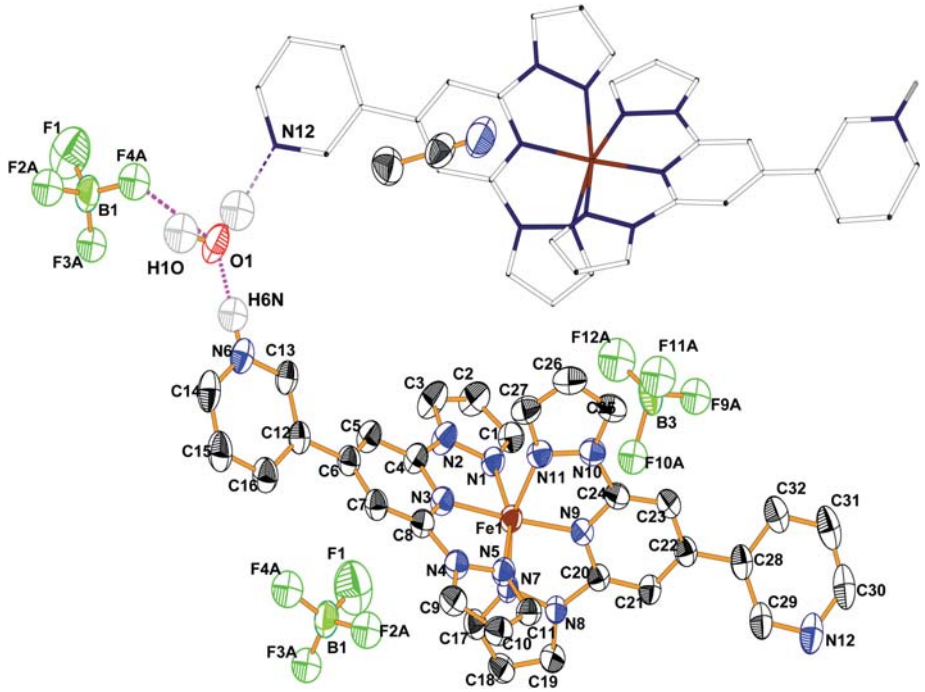

Fig. 4 ORTEP view of the crystal structure of **3** $[Fe(\mathbf{L})(\mathbf{LH})](BF_4)_3 \cdot H_2O \cdot CH_3CN$ (50% probability level of thermal ellipsoids). Bond distances of coordination polyhedron at 180(2) K (in Å): Fe1–N1 = 1.977(3), Fe1–N3 = 1.890(3), Fe1–N5 = 1.975(3), Fe1–N9 = 1.894(3), Fe1–N11 = 1.957(3). Pink dashed lines represent hydrogen bonds, O1–N6 = 2.587 Å, O1–N12 = 2.717 Å, O1–F4A = 2.699 Å.

Above room temperature the ST takes place; the χT product starts to increase gradually and at 480 K it reaches 3.06 $cm^3\ mol^{-1}$ K, which is an expected value for the high spin iron(II) compound. The measurement in cooling and heating mode does not reveal any differences and it exhibits a spin transition without any evidence of a thermal hysteresis loop.

Compound **2**, which is isostructural with compound **1**, possesses very similar spin transition properties like its perchlorate analogue **1**. The χT product at 5 K temperature is very close to zero, what clarifies the low spin state of compound at this temperature. The χT *vs.* T curve increases rather linearly in the thermal range 5–330 K (0.69 $cm^3\ mol^{-1}$ K at 330 K), which is caused either by remnant HS iron(II) fraction or by temperature-independent paramagnetism.

Above 330 K the spin transition takes place and the product function starts to increase rapidly. High-spin saturation sets in at

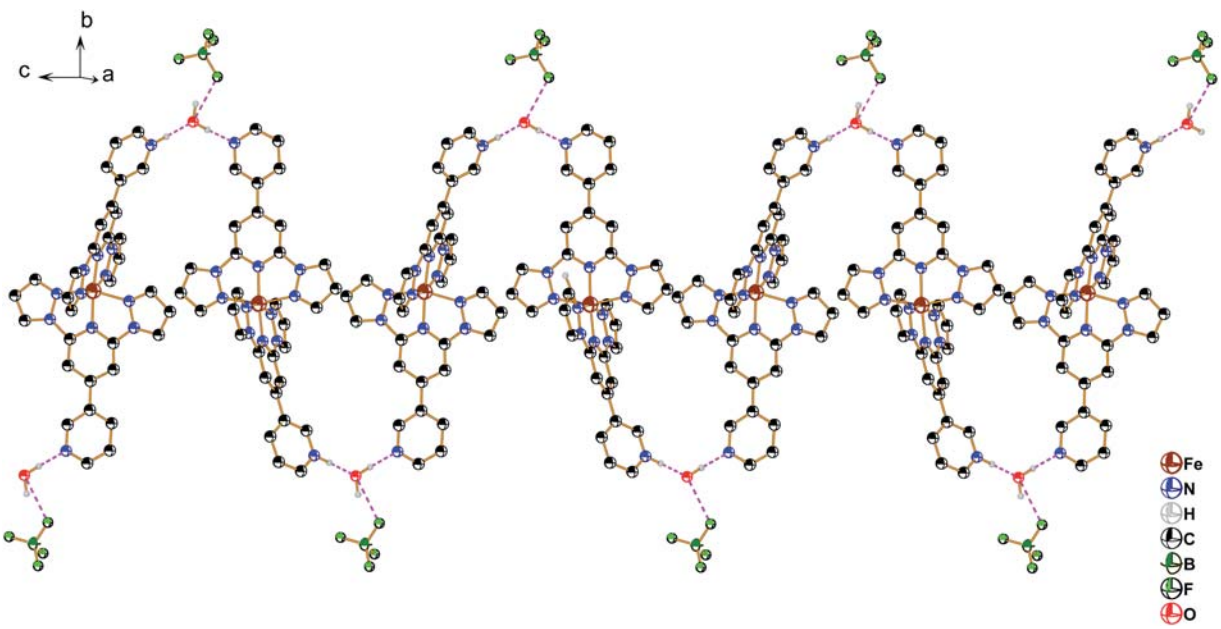

Fig. 5 1D hydrogen bonded infinite chain in the supramolecular structure of compound **3**.

Table 3 Selected angles (in °, at 180(2) K) of coordination polyhedra of compounds **1**, **2** and **3**

	1	2	3
N3–Fe1–N11	100.21(19)	100.22(12)	93.71(14)
N3–Fe1–N7	99.72(19)	99.69(12)	106.21(13)
N1–Fe1–N5	160.02(17)	160.27(11)	160.02(13)
N7–Fe1–N11	160.08(17)	160.09(11)	160.08(14)
N1–Fe1–N3	80.04(14)	80.33(11)	79.86(13)
N5–Fe1–N9	100.99(19)	100.76(11)	98.02(13)

487 K, whereby the χT product reaches 3.49 cm^3 mol^{-1} K, which is a typical value for a mononuclear high-spin iron(II) system. Also in this case, the measurements performed in heating and cooling cycles revealed that reversible spin transition without any indication of thermal hysteresis behaviour takes place. Interestingly, the variation of the counter anions does not result in a strong impact on the ST properties of the complex cations $[Fe(\mathbf{L})_2]^{2+}$; both ClO_4- and BF_4-analogues exhibit almost identical ST temperatures of $T_{1/2} = 406$ K (for compound **1**) and $T_{1/2} = 400$ K (for compound **2**).

The results of the fitting procedure are collected in Table 4 and the fitted data are displayed in Fig. 7 as solid lines. It can be concluded that the quality of the fit is satisfactory. The values of g_{HS} (2.22 and 2.36) match those expected for high-spin Fe(II) compounds. Also the averaged vibrational wavenumbers span the interval characteristic for LS (417, 269 cm^{-1}) and HS (298, 179 cm^{-1}) Fe–N modes. The cooperativeness (J) has not been ignored even for these compounds, in order to satisfactorily fit the curves. The thermodynamic parameters of the spin crossover are constrained by the equation $T_{1/2} = \Delta H/\Delta S$. Thus high values of $T_{1/2}$ (~400 K) imply high values of ΔH. The calculated values $\Delta H = 14.3$ and 19.6 kJ mol^{-1}, respectively, lie at the higher edge of experimental findings.[5] Using an approximation of:

$$r_{eff} \doteq 5(h\bar{\nu}_{LS}/h\bar{\nu}_{HS})^{15} \quad (6)$$

a rough estimate for the entropy of the transition is $\Delta S = R \ln r_{eff}$, which gives 55.4 and 64.2 J K^{-1} mol^{-1} for **1** and **2**, respectively.

Table 4 Parameters of the spin crossover[a]

	1	2	3
g_{HS}	2.22	2.36	2.25
$\alpha_{LS}/10^{-3}$ cm^3 mol^{-1}	0.64	2.06	0.06
x_{PI} (%)	5.05	2.10	1.54
Θ_{PI}/K	−1.9	−32.3	−0.20
(J/k)/K	228	250	305
(Δ_{eff}/k)/K	1727	2358	1065
$h\bar{\nu}_{LS}$/cm^{-1}	417	269	266
$h\bar{\nu}_{HS}$/cm^{-1}	298	179	177
R (%)	3.0	6.5	8.5
ΔH/kJ mol^{-1}	14.3	19.6	8.6
ΔS/J K^{-1} mol^{-1}	55.4	64.2	64.2

[a] Thermodynamic parameters: $\Delta_{eff} = \Delta_0 + (h\bar{\nu}_{HS} - h\bar{\nu}_{LS})(3n - 6)/2$, $n = 15$, $\Delta H = R(\Delta_{eff}/k)$, $r_{eff} \doteq 5(h\bar{\nu}_{LS}/h\bar{\nu}_{HS})^{3n-6}$, $\Delta S = R \ln r_{eff}$.

Compound **3** exhibits a lattice-solvent controlled spin transition. Variable temperature magnetic investigations of the solvated compound **3** $[Fe(\mathbf{L})(\mathbf{LH})](BF_4)_3 \cdot H_2O \cdot CH_3CN$ were recorded in temperature range 5–380 K in the heating mode only (Fig. 7). The value of χT product in temperature range 5–200 K is constant and close to zero and corresponds to the low-spin state of iron(II). Above 250 K the product function starts to increase dramatically and reaches at 326 K a plateau value with 3.32 cm^3 mol^{-1} K in accordance with the expected value for the high-spin Fe(II) centre.

However, due to the liberation of water molecules from the crystal structure, this ST is irreversible. As is mentioned above, the solvent-free compound **3d** was prepared *in situ* during the recording of magnetic data. The magnetic investigation of the solvent-free sample **3d** was carried out in the temperature range 5–380 K reveals an abrupt and complete ST (Fig. 7). In the temperature region 5–225 K the value of the χT product is constant and close to zero indicating the low-spin state. Above this temperature, the thermally induced reversible ST takes place and the measurement performed in cooling and heating mode revealed significant differences in magnetic moment behaviour confirming a 9 K thermal hysteresis loop ($T_{1/2(\uparrow)} = 240$ K and $T_{1/2(\downarrow)} = 231$ K). The high-spin saturated value at 300 K is

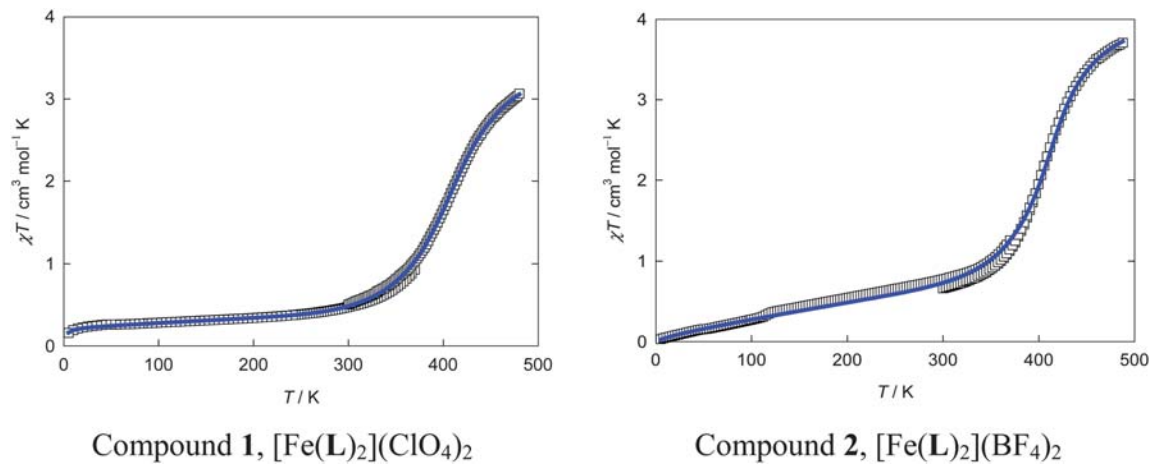

Fig. 6 Temperature dependence of the χT product of **1** and **2**. Solid lines—fitted.

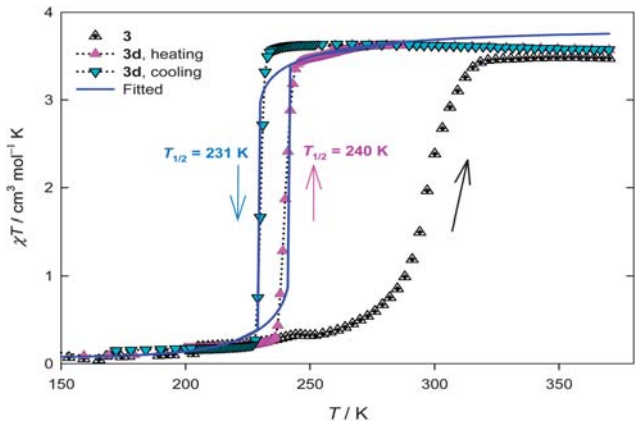

Fig. 7 Temperature dependence of the χT product of solvated compound **3** [Fe(**L**)(**LH**)]$(BF_4)_3 \cdot H_2O \cdot CH_3CN$ (crossed triangles up) and desolvated compound **3d** [Fe(**L**)(**LH**)]$(BF_4)_3$ (triangles up, triangles down). Desolvation of **3** was obtained *in situ* within the magnetic measurement, by four continuous cooling/heating cycles and maintaining the sample in the magnetometer at 380 K for 200 min before every cooling/heating cycle, until the last and next to last measurement cycle were identical.

3.61 cm^3 mol^{-1} K, an expected value for high-spin iron(II) mononuclear compounds.

The fitting procedure gave the parameters listed in Table 4 and the transition curve is displayed in Fig. 7. It can be concluded that the quality of the fit is satisfactory. The parameters of the spin crossover again sound reasonable: $g_{HS} = 2.25$, $h\bar{\nu}_{LS} = 266$ cm^{-1}, $h\bar{\nu}_{HS} = 177$ cm^{-1}, $\Delta H = 8.6$ kJ mol^{-1}, and $\Delta S = 64.2$ J K^{-1} mol^{-1}. As the cooperativeness $J/k = 305$ K overreaches the transition temperature, the hysteresis occurs.

Conclusion

In conclusion, the results presented illustrate the effect of removal of auxiliary lattice-solvent molecules on the magnetic spin transition parameters. Investigating three structurally very similar mononuclear $[Fe(\mathbf{L})_2]^{2+}$ spin transition systems, the supramolecular inclusion of lattice-solvent molecules leads to dramatically different spin transition properties, while changing the nature of the anions (from perchlorate to tetrafluoroborate) does not show any pertinent impact. The investigation shows that the control of the lattice-solvent molecules can be used in the design of technologically attractive spin transition devices.[12]

Notes and references

1 O. Kahn and C. Jay Martinez, *Science*, 1998, **279**, 44.
2 O. Kahn, J. Krober and C. Jay, *Adv. Mater.*, 1992, **4**, 718.
3 *Topics In Current Chemistry*, ed. P. Gütlich and H. A. Goodwin, Springer Verlag, Berlin–Heidelberg–New York, 2004, vol. 233–235.
4 R. N. Muller, E. L. Vander and S. Laurent, *J. Am. Chem. Soc.*, 2003, **125**, 8405.
5 I. Šalitroš, T. Madhu, R. Boča, J. Pavlik and M. Ruben, *Monatsh. Chem.*, 2009, **140**, 695.
6 (*a*) J. Kroeber, J. P. Audiere, R. Claude, E. Codjovi, O. Kahn, J. G. Haasnoot, F. Groliere, C. Jay and A. Bousseksou, *Chem. Mater.*, 1994, **6**, 1404; (*b*) F. Armand, C. Badoux, P. Bonville, A. Ruaudel-Teixier and O. Kahn, *Langmuir*, 2003, **11**, 3467; (*c*) A. Michalowicz, J. Moscovici, B. Ducourant, D. Cracco and O. Kahn, *Chem. Mater.*, 1995, **7**, 1833; (*d*) E. Codjovi, L. Sommier and O. Kahn, *New J. Chem.*, 1996, **20**, 503; (*e*) C. Cantin, H. Daubric, J. Kliava, J. Servant, J. Sommier and O. Kahn, *J. Phys.: Condens. Matter*, 1998, **10**, 7057; (*f*) E. Coronado, J. R. Galán-Mascarós, M. Monrabal-Capilla, J. García-Martinéz and P. Pardo-Ibañéz, *Adv. Mater.*, 2007, **19**, 1359.
7 (*a*) V. Niel, J. M. Martinez-Agudo, M. C. Muñoz, A. B. Gaspar and J. A. Real, *Inorg. Chem.*, 2001, **40**, 3838; (*b*) S. Bonhommeau, S. Molnár, A. Galet, A. Zwick, J. A. Real, J. J. McGarvey and A. Bousseksou, *Angew. Chem., Int. Ed.*, 2005, **44**, 4069; (*c*) A. Larionova, L. Salmon, Y. Guari, A. Tokarev, K. Molvinger, G. Molnár and A. Bousseksou, *Angew. Chem., Int. Ed.*, 2008, **47**, 8236; (*d*) S. Cobo, S. Molnár, S. Real and S. Bousseksou, *Angew. Chem., Int. Ed.*, 2006, **45**, 5786; (*e*) I. Boldog, I. Gaspar, V. Marinez, P. Pardo-Ibañéz, V. Ksenofontov, A. Bhattacharje, P. Gütlich and J. A. Real, *Angew. Chem., Int. Ed.*, 2008, **47**, 6433.
8 (*a*) J. M. Holland, J. A. McAllister, Z. Lu, C. A. Kilner, M. Thornton-Pett and M. A. Halcrow, *Chem. Commun.*, 2001, 577; (*b*) C. Rajadurai, Z. Qu, Z. Fuhr, Z. Gopalan, R. Kruk, M. Ghafari and M. Ruben, *Dalton Trans.*, 2007, 3531; (*c*) C. Rajadurai, F. Schramm, O. Fuhr and M. Ruben, *Eur. J. Inorg. Chem.*, 2008, 2649; (*d*) C. Rajadurai, O. Fuhr, R. Kruk, M. Ghafari, M. Hahn and M. Ruben, *Chem. Commun.*, 2007, 2636; (*e*) N. T. Madhu, I. Šalitroš, F. Schramm, S. Klyatskaya, O. Fuhr and M. Ruben, *C. R. Chim.*, 2008, **11**(10), 1166; (*f*) C. Rajadurai, F. Schramm, S. Brink, O. Fuhr, M. Ghafari, R. Kruk and M. Ruben, *Inorg. Chem.*, 2006, **45**, 10019; (*g*) E. Coronado, M. C. Giménez-López, C. Giménez-Saiz and F. M. Romero, *CrystEngComm*, 2009, **11**, 2198.
9 (*a*) R. Boča, M. Boča, L. Dlháň, K. Falk, H. Fuess, W. Haase, R. Jaroščiak, R. Papánková, F. Renz, M. Vrbová and R. Werner, *Inorg. Chem.*, 2001, **40**, 3025; (*b*) R. Boča, F. Renz, F. Boča, H. Fuess, W. Haase, G. Kickelbick, W. Linert and M. Vrbová-Schikora, *Inorg. Chem. Commun.*, 2005, **8**, 227.
10 G. M. Sheldrick, *Acta Crystallogr., Sect. A: Fundam. Crystallogr.*, 2008, **64**, 112.
11 (*a*) R. Boča and W. Linert, *Monatsh. Chem.*, 2003, **134**, 199; (*b*) A. Bousseksou, H. Constant-Machado and F. Varret, *J. Phys. I*, 1995, **15**, 747; (*c*) R. Boča, *Program Polymagnet-06*, Slovak University of Technology, Bratislava, 2006.
12 (*a*) M. Cavallini, I. Bergenti, I. Milita, G. Ruani, I. Salitros, Z.-R. Qu, R. Chandrasekhar and M. Ruben, *Angew. Chem., Int. Ed.*, 2008, **47**, 8596; (*b*) M. Ruben, A. Landa, A. Lörtscher, A. Riel, M. Mayor, H. Görls, H. B. Weber, H. B. Arnold and F. Evers, *Small*, 2008, **4**, 2229; (*c*) C. Rajadurai, F. Schramm, O. Fuhr and M. Ruben, *Eur. J. Inorg. Chem.*, 2008, 2649; (*d*) P. D. Southon, L. Liu, E. A. Fellows, D. J. Price, G. J. Halder, K. W. Chapman, B. Moubaraki, K. S. Murray, J.-F. Letard and C. J. Kepert, *J. Am. Chem. Soc.*, 2009, **131**, 10998; (*e*) M. Ohba, K. Yoneda, G. Augst, M. C. Munoz, A. B. Gaspar, J. A. Real, M. Yamasaki, H. Ando, Y. Nakao, S. Sakaki and S. Kitagawa, *Angew. Chem., Int. Ed.*, 2009, **48**, 4767; (*f*) M. Quesada, V. A. de la Pena-O'Shea, G. Aromi, S. Geremia, C. Massera, O. Roubeau, P. Gamez and J. Reedijk, *Adv. Mater.*, 2007, **19**, 1397.

